MBE GROWN GAINNAS SOLAR CELLS FOR MULTIJUNCTION APPLICATIONS

David Jackrel, Homan Yuen, Junxian Fu, Seth Bank, Xiaojun Yu, Zhilong Rao, and James S. Harris
Stanford University, Stanford, CA 94305

ABSTRACT

Triple-junction cells composed of III-V materials currently hold the world record for photovoltaic efficiency. [1] In order to further increase cell efficiency in the future 4- and 5- junction cells incorporating a sub-cell with a bandgap of roughly 1.0 eV will be required. In this study 1.0 eV bandgap GaInNAs devices grown by solid source molecular beam epitaxy are investigated in terms of materials quality and device performance that show similar or better properties to the best MOVPE grown devices found in the literature. Deep-level transient spectroscopy measurements illustrate that the trap concentrations in the GaInNAs material are significantly lower than that of MOVPE grown material. [2-4] The internal quantum efficiency (43%), open-circuit voltage (450 mV), short-circuit current density (25.76 mA/cm^2) and fill-factor (56.4%) of the GaInNAs devices under 1-sun power density 1064 nm radiation are similar to or surpass the properties of the best MOVPE GaInNAs devices found in the literature. [5]

INTRODUCTION

Multijunction photovoltaic cells are necessary to obtain the highest cell efficiencies. The current world record photovoltaic cell, produced by Spectrolab, is a triple junction structure composed of GaInP/GaAs/Ge with a power conversion efficiency of over 37%. [6] In order to further maximize the power conversion of the solar spectrum the collected light must be spilt into smaller wavelength regions through the use of 4- and 5-junction cells. The optimization of these multijunction cells requires a sub-cell with a bandgap between that of Ge (0.66 eV) and GaAs (1.42 eV). One material that is particularly attractive is the dilute nitride GaInNAs which has a tunable bandgap near 1.0 eV and can be grown lattice-matched to GaAs substrates.

GaInNAs photovoltaic cells have historically been plagued with low conversion efficiencies due to small open-circuit voltages and low short-circuit currents caused by short carrier lifetimes leading to short diffusion lengths. [7] The current alternative to reach the 1.0 eV bandgap is to employ InGaAs materials which are significantly lattice-mismatched to GaAs. Historically metamorphic InGaAs devices have low conversion efficiencies due to dislocations originating in the graded buffer layer and subsequently threading into the active region of the devices. (Figure 1) Recently metamorphic devices have been produced with significantly reduced Shockley-Read-Hall recombination rates and efficiencies approaching those of lattice-matched cells. [6] However maintaining the lattice-matching through the entire structure has the potential to improve the materials quality in the upper sub-cells due to the absence of the highly dislocated region inevitable in metamorphic devices.

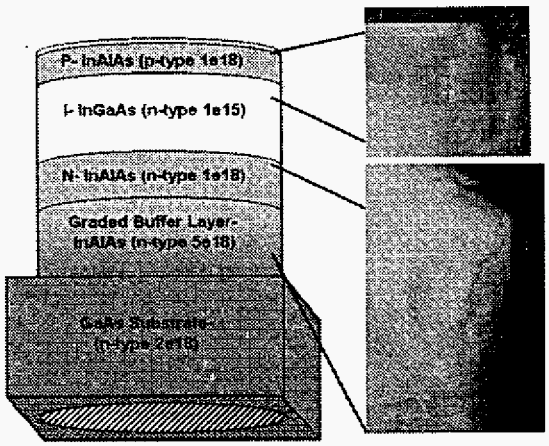

Fig. 1. Metamorphic-InGaAs structure and TEM images

Dilute nitride GaInNAs material can be grown using metalorganic vapor phase epitaxy (MOVPE) or solid source molecular beam epitaxy (MBE) with nitrogen supplied by a RF-plasma source. MBE has advantages over MOVPE due to the absence of hydrogen and in the control of the nitrogen incorporation in GaInNAs, and has produced the best quality material to date in the effort to produce 1 eV photovoltaic cells [7] and long-wavelength 1550 nm lasers for telecommunications. [8,9]

EXPERIMENT

Lattice-matched GaInNAs double-heterostructure PIN devices were grown on (100) GaAs substrates using solid source MBE with a nitrogen RF-plasma source. The intrinsic GaInNAs material is 1-2 microns thick, composed of approximately 1% N, and has a p-type doping of roughly 10^{16} cm^{-3}. The N- and P- barrier layers were composed of GaAs. These structures were processed into rear-illuminated devices with active areas 3 mm in diameter. The rear-illuminated structures have the intrinsic

0-7803-8707-4/05/$20.00 ©2005 IEEE.

layers directly adjacent to ceramic heat sinks and therefore have excellent thermal conductivities. The materials properties and device performance were then characterized and compared to metamorphic InGaAs material and other GaInNAs devices in the literature.

Surface roughness characterization was performed using a Zygo interferometric white light 3-D surface profiler. X-ray diffraction measurements were performed using a Phillips X'Pert PRO diffractometer. Time-resolved photoluminescence was done at NREL by Wyatt Metzger using time-correlated single-photon counting. Fourier Transform deep-level transient spectroscopy was performed at Accent Optical. Photocurrent and quantum efficiency measurements were performed with a 1064 nm Nd:YAG NPRO laser from Lightwave, and a Hewlett-Packard 4186A semiconductor parameter analyzer.

RESULTS AND DISCUSSION

Materials Characterization

The use of a linearly graded buffer layer in lattice-mismatched structures confines the misfit dislocations away from the active region of the device. However, all of the strain is not compensated for by the misfit dislocations; some strain is relieved by the conglomeration of misfit dislocations along [110] directions resulting in 3-D surface oscillations. [10] The surface roughness of the metamorphic InGaAs structures was found to be roughly an order of magnitude rougher than the lattice-matched GaInNAs structures. (Figure 2) The RMS roughness of the GaInNAs film is 0.78 nm while the metamorphic film is 6.16 nm.

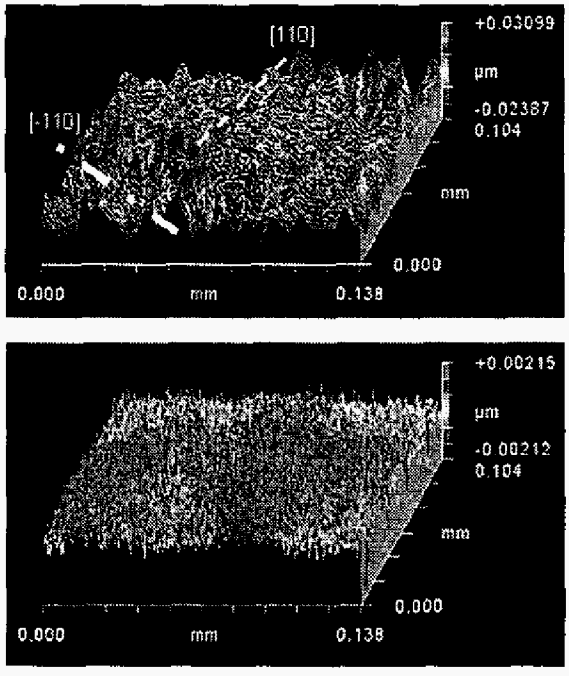

Fig. 2. MM-InGaAs and LM-GaInNAs surface roughness

X-ray diffraction reciprocal space maps were performed to ensure that the lattice-matched material was coherent to the GaAs substrate. Figure 3A shows the InGaAs and InAlAs layers in a metamorphic structure occur along the omega/2-theta direction indicating relaxation, while figure 3B shows the GaInNAs peak slightly strained but remaining completely coherent to the GaAs substrate. The diffuse peak between the substrate and film layers in the metamorphic structure is due to the changing lattice constant in the graded buffer layer.

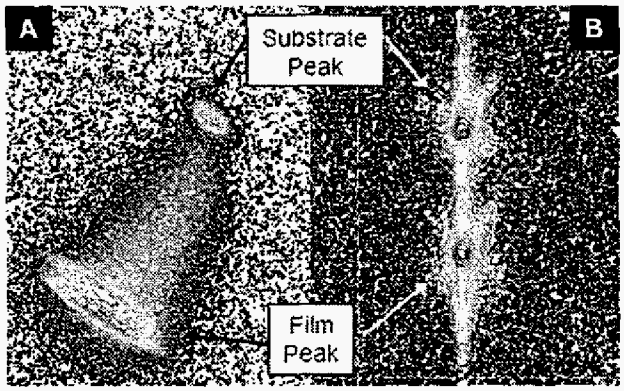

Fig. 3. A. MM-InGaAs and B. LM-GaInNAs XRD reciprocal space maps

X-ray rocking curves of both structures are shown in figure 2 plotted on the same omega/2-theta scale. The lattice constant of the GaInNAs material is very close to that of GaAs and thus can be grown coherently on GaAs substrates while the lattice-mismatch between the InGaAs and GaAs materials is more than 1.5% which necessitates the incorporation of the graded buffer. It can also be noted that the FWHM of the layer peak in the InGaAs material is much larger than the GaInNAs material due to rotation of the crystal planes resulting from interface roughening and materials defects.

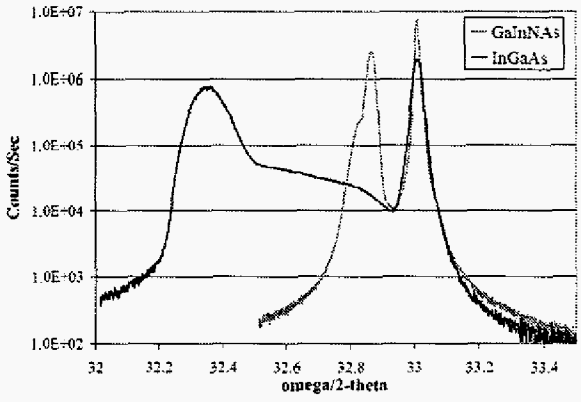

Fig. 4. MM-InGaAs and LM-GaInNAs XRD rocking curves

Photoluminescence (PL) measurements were performed to probe the bandgap as well as the relative amount of radiative recombination in the GaInNAs materials. (Figure 5) The GaInNAs structures were annealed at various temperatures to reduce the number of non-radiative defects present in the as-grown (AG) material which quench the PL intensity. The optimal annealing temperature was found to be 860°C, above which the PL intensity began to drop due to thermal damage. Time-resolved PL measurements also show an increased carrier lifetime with higher annealing temperatures. (Figure 6) The improved carrier lifetime is most likely due to both a reduction in the defect density as well as a reduction in the compositional inhomogeneity common in dilute nitrides.

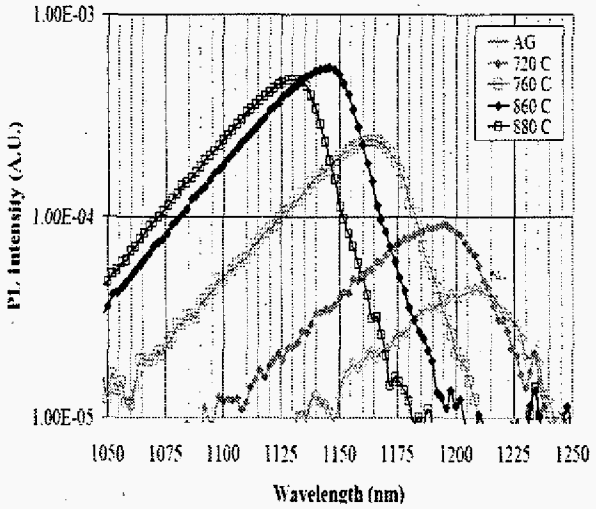

Fig. 5. Photoluminescence spectra of GaInNAs at different annealing temperatures

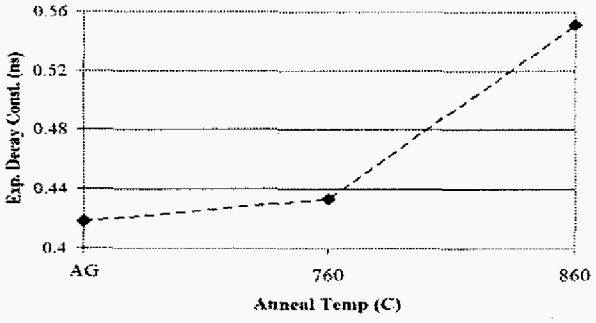

Fig. 6. Time-resolved photoluminescence decay constants of GaInNAs at different annealing temperatures

Device Optoelectronic Characterization

Deep-level transient spectroscopy is a powerful technique for directly observing non-radiative defect centers in semiconductor device structures. Majority carrier hole traps were observed in the p-type GaInNAs material at activation energies of 0.63 eV, 0.27 eV, 0.22 eV, and 0.15 eV above the valence band edge, with the largest concentration at 0.63 eV. These values are fairly consistent with values from the literature. (Table 1) For instance Balcioglu et al. have reported hole traps in GaInNAs at 0.59 eV with a density of 5.6×10^{14} cm^{-3}, and Johnston, et al. have reported hole traps at 0.13 eV with a density of 1.4×10^{14} cm^{-3}. [2-4] However, the trap concentrations in the GaInNAs materials in this study are all 3-10 times lower than in the MOVPE-grown materials from other studies.

Sample	Activation Energy (eV)	Trap Density (cm^{-3})	Capture Cross-Section (cm^2)
GaInNAs - This work	0.63	1.1×10^{14}	9.0×10^{-15}
	0.27	3.9×10^{13}	2.5×10^{-16}
	0.22	7.5×10^{13}	3.2×10^{-15}
	0.15	1.7×10^{13}	5.2×10^{-18}
GaInNAs - Other studies	0.79 [2]	3.9×10^{14}	1.1×10^{-12}
	0.59 [3]	5.6×10^{14}	9.1×10^{-14}
	0.23 [4]	3.8×10^{14}	-
	0.13 [2]	1.4×10^{14}	5.0×10^{-15}

Table 1. Deep-level transient spectroscopy data from GaInNAs majority-carrier traps

Figure 7 shows the IV response of a GaInNAs device under 1064 nm illumination with roughly 1-sun power density (100 mW/cm^2). The short-circuit current was 25.8 mA/cm^2 and the open-circuit voltage was 450 mV. The internal quantum efficiency at 1064 nm was 43% and the fill factor at 1-sun power density was 56.4%. The maximum power conversion efficiency of the 1064 nm single wavelength illumination was about 10%, which would correspond to greater than 5% efficiency under AM1.5 solar illumination. (Figure 8) These values surpass the best results from MOVPE grown GaInNAs devices reported in the literature. [5]

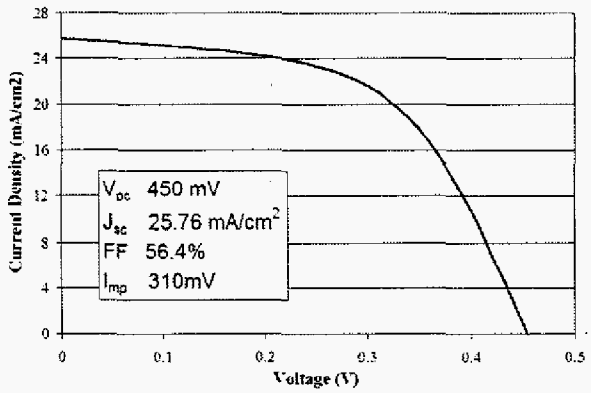

Fig. 7. GaInNAs device current density under 1-sun power density (100 mW/cm^2) 1064 nm illumination

The conversion efficiencies are considerably lower than the best metamorphic InGaAs cells partially due to

the low open-circuit voltage and partially to the low fill factors. [11] These problems can be attributed to short carrier lifetimes leading to short majority and minority carrier diffusion lengths. Although the material was optimized by post-growth annealing, there is still some optimization of the material that can be undertaken during growth. Recent advances have been developed to reduce the number of defects present in MBE grown GaInNAs by utilizing biased deflection plates to protect the growth surface from ion damage. Furthermore, elemental Sb acts as a surfactant during growth of GaInNAs(Sb) which can reduce the defects and compositional inhomogeneity. [12] The next generations of dilute nitride photovoltaic cells that we investigate will employ one or both of these methods in the hope of improving carrier lifetimes and device performance.

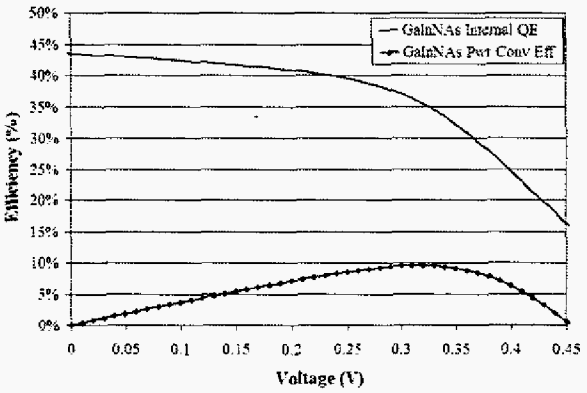

Fig. 8. GaInNAs device internal quantum efficiency and power conversion efficiency under 1-sun power density (100 mW/cm^2) 1064 nm illumination

SUMMARY

GaInNAs devices grown using MBE with properties surpassing the best published MOVPE cells are reported. Surface roughness measurements show that the lattice-matched material has significantly reduced roughness compared to metamorphic materials. Annealing studies were performed to optimize the material after growth which increased the photoluminescence intensity and carrier lifetimes. Deep-level transient spectroscopy measurements illustrate that the trap concentrations in the GaInNAs material are significantly lower than that of MOVPE grown material. The internal quantum efficiency, open-circuit voltage and short-circuit current of the GaInNAs devices under 1-sun power density 1064 nm radiation are reported.

REFERENCES

[1] M.A. Green, K. Emery, D.L. King, S. Igari, and W. Warta, "Solar Cell Efficiency Tables (Version 24)", *Prog. Photovolt: Res. Appl.* **12**, 2004, pp. 365-372.

[2] S.W. Johnston, R.K. Ahrenkiel, D.J. Friedman and S.R. Kurtz, "Deep-Level Transient Spectroscopy in InGaAsN Lattice-Matched to GaAs", *Twenty-Ninth IEEE PVSC*, 2002, pp. 1023-1026.

[3] A. Balcioglu, R.K Ahrenkiel, D.J. Friedman, "Effects of Oxygen Contamination on Diffusion Length in P+-N GaInNAs Solar Cells", *J. Appl. Phys.* **93**, 2003, pp. 3635-3642.

[4] D. Kwon, R.J. Kaplar, S.A. Ringel, A.A. Allerman, S.R. Kurtz, and E.D. Jones, "Deep Levels in P-Type InGaAsN Lattice Matched to GaAs", *Appl. Phys. Lett.* **74**, 1999, pp. 2830-2832.

[5] Baur, C. et al., "Development of a 1.0 eV (GaIn)(NAs) Solar Cell", *3rd World Conf. on Photovolt. Energy Conversion*, 2003, pp. 677-680.

[6] R.R King et al., "Metamorphic III-V Materials, Sublattice Disorder, and Multijunction Solar Cell Approaches with Over 37% Efficiency", *Presented at the Nineteenth European Photovolt. Solar Energy Conf.*, 2004.

[7] D.J. Friedman, J.F. Geisz and A.J. Ptak, "Photovoltaic Applications of Dilute Nitrides", *Optoelectronic Properties of Semiconductors and Superlattices, Vol. 21: Physics and Applications of Dilute Nitrides, I.A. Buyanova and W.M. Chen* (Taylor and Francis, New York, 2004), pp. 371-393.

[8] S. Bank, M.A. Wistey, L.L. Goddard, H.B. Yuen, V. Lordi and J.S. Harris, "Low-Threshold Continuous-Wave 1.5μm GaInNAsSb Lasers Grown on GaAs", *IEEE J. of Quantum Electron.* **40**, 2004, pp. 656-664.

[9] J.S. Harris, "GaInNAs and GaInNAsSb Long-Wavelength Lasers", *Optoelectronic Properties of Semiconductors and Superlattices, Vol. 21: Physics and Applications of Dilute Nitrides, I.A. Buyanova and W.M. Chen* (Taylor and Francis, New York, 2004), pp. 395-433.

[10] F. Romanato et al., "Strain Relaxation in Graded Composition $In_xGa_{1-x}As$/GaAs Buffer Layers", *J. Appl. Phys.* **86**, 1999, pp. 4748-4755.

[11] F. Dimroth, P. Lanyi, U. Schubert and A.W. Bett, "MOVPE Grown $Ga_{1-x}In_xAs$ Solar Cells for GaInP/GaInAs Tandem Applications", *J. Electron. Mater.* **29**, 2000, pp. 42-46.

[12] V. Gambin, W. Ha, M. Wistey, H. Yuen, S.R. Bank, S.M. Kim and J.S. Harris, "GaInNAsSb for 1.3-1.6 μm Long Wavelength Lasers Grown by MBE", *IEEE J. of Select. Topics Quantum Electron.* **8**, 2002, pp. 795-800.